PHYSICAL REVIEW B **78**, 155103 (2008)

Charge and orbital ordered phases of $La_{2-2x}Sr_{1+2x}Mn_2O_{7-\delta}$

H. Zheng, Qing'An Li, K. E. Gray, and J. F. Mitchell
Materials Sciences Division, Argonne National Laboratory, Argonne, Illinois 60439, USA
(Received 30 June 2008; published 3 October 2008)

Our studies have significantly modified the conventionally held view of the phase diagram of $La_{2-2x}Sr_{1+2x}Mn_2O_{7-\delta}$ for two compositions exhibiting charge (and orbital) order (CO), i.e., at hole-doping levels, $h=x-\delta$, of ~ 0.5 and ~ 0.6. These CO states are stable over very narrow doping ranges ($\Delta h \sim \pm 0.005$) at the lowest temperatures, but those ranges increase at higher temperatures (to $\Delta h \sim \pm 0.02$) in a manner consistent with simple entropy considerations. Such narrow ranges dictate the crucial need for crystal homogeneity. Attesting to such homogeneity is a conductivity ratio of $>10^{10}$ upon crossing the first-order phase boundary from CO at $h=0.60$ to A-type antiferromagnetic (AAFM) at $h\sim 0.59$ or $h\sim 0.61$ plus two findings that were missed in the existing literature: that these CO phases are the ground state at the lowest temperatures, and for $h\sim 0.5$, that coexistence of the CO and AAFM phase is absent at any temperature.

DOI: 10.1103/PhysRevB.78.155103 PACS number(s): 75.30.Et, 75.60.−d

Reduced dimensionality can aid the quest to better understand strongly correlated electrons since its reduction of the mean-field ordering temperature can expose competing interactions through more prominent fluctuations. For manganites[1] there is a vigorous competition among orbital, charge, and spin order; and in bilayer compounds,[2] $La_{2-2x}Sr_{1+2x}Mn_2O_{7-\delta}$, this competition is readily apparent in the fluctuations seen in the paramagnetic (PM) insulator phases above their ordering temperatures.[3] For example the PM phase for hole doping, $h=x-\delta\sim 0.4$, reveals charge[4] and polaronic[5] fluctuations competing with ferromagnetic (FM) spin fluctuations[6] that eventually win out at its Curie point. The backbone of such scientific inquiry is to establish the ground states across the accessible range of h that include[3] fully FM spin order, two versions of A-type antiferromagnetic (AAFM) order (FM monolayers with AFM orientation within the bilayer and for $h\sim 0.3$, FM bilayers with AFM orientation between them), charge and orbital ordered (CO) states ("checkerboard" ordering with the CE-type magnetic order[7] for $h\sim 0.5$ and more complex CO for $h\sim 0.6$ and ~ 0.67), and a variety[3] of other types of AFM order for $h>0.67$.

Here we emphasize the narrow, needlelike regions in the phase diagram of Fig. 1: the CO phase at $h\sim 0.5$ was reported previously[8] and we now report a systematic study for the CO phase found for $h\sim 0.6$. These CO phases appear to interrupt and replace the "background" AAFM that otherwise would exist continuously from $h\sim 0.48$ to at least $h\sim 0.61$. Previous to Ref. 8, it had been commonly accepted that CO at $h=0.5$ was re-entrant,[9–15] forming below ~ 210 K, but then being replaced by an AAFM below ~ 100 K. This lack of a low-temperature CO ground state was surprising as it is found at $h=0.5$ in many perovskite manganites.[16] In bilayer manganites, coexistence of CO and AAFM between ~ 100 and ~ 200 K had also been universally reported.[9–12,14] To reveal the intrinsic behavior[8] required a high degree of crystal homogeneity that was verified through the use of multiterminal transport measurements (see the Appendix) that critically evaluate homogeneity and provide feedback to crystal growth. Such results for $h\sim 0.5$ showed that the CO phase does exist at low temperatures and no coexistence was found.[8]

The following (1) presents experiments that systematically map the qualitative features of the needlelike phase for $h\sim 0.6$; (2) presents experiments directly addressing oxygen nonstoichiometry; (3) presents a simplified entropy argument to support the qualitative shape of the needlelike phases; (4) reports the transport properties of pure CO crystals at $h=0.6$; and (5) frames some unanswered questions exposed by new features in the modified phase diagram.

A review of our methodology to provide adequate crystal homogeneity is given in the Appendix, but it is important to emphasize that homogeneity is a separate issue from abso-

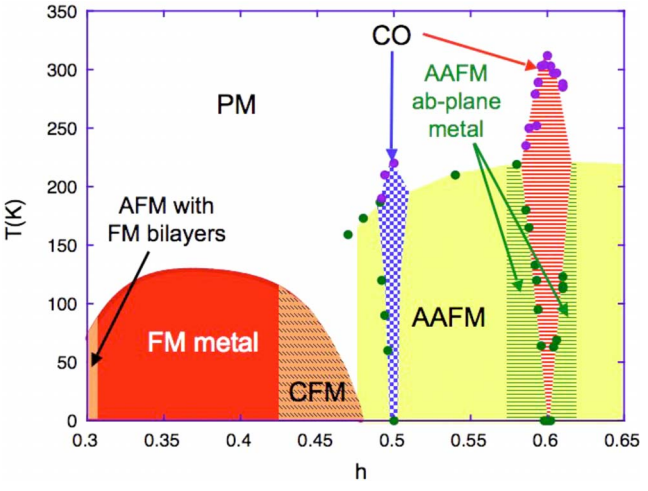

FIG. 1. (Color online) Modified phase diagram for the bilayer manganite, $La_{2-2x}Sr_{1+2x}Mn_2O_7$. The needlelike CO phase at $h=x-d=0.5$ was reported recently (Ref. 8) and that for the CO phase at 0.6 is reported here. The *ab*-plane-metallic *A*-type AFM phase occurs at (Ref. 24) $h\sim 0.58$ and (Ref. 19) $h\sim 0.59$ and here reported for $h\sim 0.61$. The upper limit of h for this *ab*-plane metal is unknown and the lower limit is poorly known. The previously reported bilayer phases for $h<0.48$, FM metal, canted FM (CFM), and AFM-oriented FM bilayers, are indicated for completeness. We presently have insufficient data to establish the potentially interesting detailed behavior in the vicinity of $h\sim 0.46$, where the FM metallic and AAFM insulator phases collide, or near $h\sim 0.55$ or for $h>0.61$.

lute hole-doping level, h. For a nominal Sr doping in the polycrystalline feed rod, x_0 (an obvious abbreviation for the actual Sr content per formula unit, $1+2x_0$), the first crystallization in the floating zone is known[17] to occur at $x<x_0$ for $La_{2-2x}Sr_{1+2x}Mn_2O_{7-\delta}$. In the following, we assume there are no instabilities during growth; then x rises and settles to x_0 by the central part of the boule, and if growth is continued to the end of the feed rod, the last zone length will compensate with $x>x_0$. Thus, x_0 is inadequate for determining the Sr doping, x, of individual crystals extracted from the boule. It is especially unreliable if growth instabilities interrupt the above scenario, but variable oxygen nonstoichiometry, δ, could also contribute to uncertainties in $h=x-\delta$. Consistent with our own experience, the reports of others[9–15,18] show widely variable properties for nominal "$x_0=0.5$." Considering the precision on h that is needed, we have not found adequate nondestructive, or even destructive, quantitative analyses (e.g., energy dispersive x-ray spectroscopy and inductively coupled plasma-atomic emission spectroscopy are accurate to 2–3% at best). Thus only a qualitative hole-doping scale, based on the measured physical properties, was used in Ref. 8. Due to the difficulty of quantifying h and x, in our samples, or those in literature, the following nomenclature will be adopted. Clearly by x_0 we mean the starting or nominal composition of the boule, and it is the only information we have for data from the literature and many of our crystals. The actual x is most likely smaller than, but certainly not greater than, x_0 for stable growth. As our slow-cool protocol precludes negative δ, the actual h is most likely smaller than, but not greater than, x. Our use of h, x, or x_0 throughout the paper reflects either the most physically relevant one for the discussion at hand or the "best"—or only—known value. We now discuss our control of x and δ in turn.

A compelling realization of the qualitative doping-dependent phase diagram of CO states is reported here for $h\sim h_{CO}=0.6$, even if it is still only semiquantitative. In this experiment, the nominal Sr composition, x_0, of the polycrystalline feed rod was 0.61, and growth proceeded without instabilities until a crack formed near the very end. Eleven samples were extracted from various positions along the resulting boule (see top of Fig. 2) and their transitions measured by magnetization. In earlier works we showed[8,19] the equivalence of magnetization, transport, and x rays for identifying CO. Such transition temperatures are plotted in Fig. 2 as a linear function of crystal number (1–11) and not distance along the boule. The data that precede these on the plot came from two samples extracted[19] from a boule with $x_0=0.60$, and they have been assigned a qualitative position based on their transition temperatures. An additional data point for $x_0=0.58$ shows a single, direct transition from PM to AAFM. The abscissa of Fig. 2 is clearly a qualitative scale of h, but some fixed points can be assigned. The final three samples (9–11) exhibit barely distinguishable transition temperatures and span about a third of the boule length. It is reasonable to assign these to $x=x_0=0.61$, while the three samples (4–6) that do not show the AAFM phase at low temperature are strongly expected to represent the CO state centered at $h_{CO}=0.60$.

Then based on the data of Fig. 2, one can imagine that crystals reported in literature may be inadvertently underdoped, i.e., x less than the nominally quoted x_0. The amount of underdoping, which can be as much as 0.02 or possibly more, is estimated from the data of Fig. 2 for $h\sim 0.6$ by assuming a reasonably symmetric effect on transition temperatures with $|h-h_{CO}|$. Extrapolating this trend to nominal "$x_0=0.5$" doping could begin to explain the widely variable properties reported,[8–15,18] and why, if the initial part of the boule were used, the resulting range of doping could simulate coexistence.

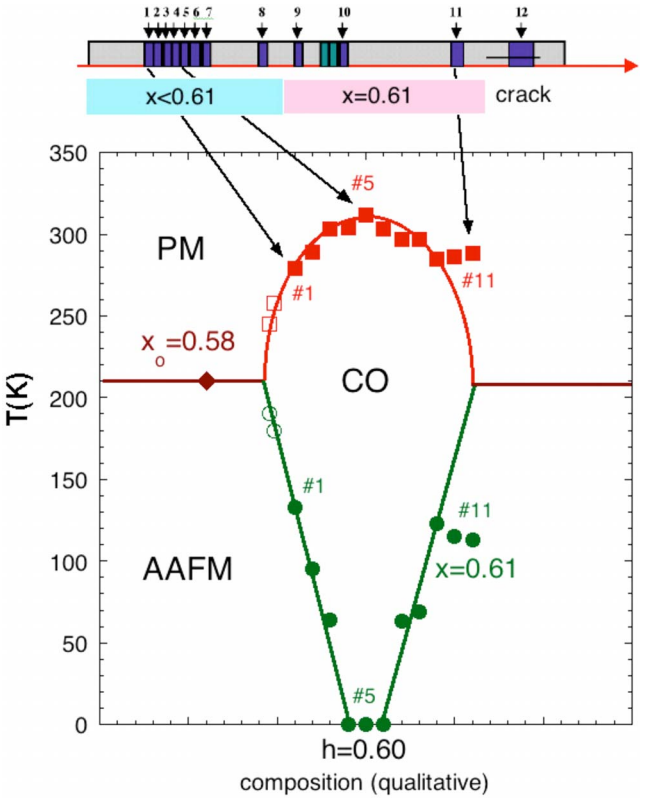

FIG. 2. (Color online) Schematic, *qualitative* phase diagram near $h=0.6$. Symbols are measured transition temperatures (squares represent PM insulator to CO state; circles represent CO state to AAFM) taken at various positions along a boule (top drawing) of nominal composition $x_0=0.61$. They are plotted as a linear function of crystal number and not distance along the boule. Crystals 9 through 11 exhibit indistinguishable transitions and are anticipated to be at the same value of $x=x_0=0.61$. Additional data come from crystals made of a nominally $x_0=0.60$ boule (unfilled symbols placed at positions suggested by their transition temperatures) and $x_0=0.58$ boule (filled diamond that is a direct transition from PM to AAFM).

We now address oxygen nonstoichiometry. The bilayer manganites seem to be far less susceptible to oxygen nonstoichiometry than perovskite manganites, and recent studies find[20] for polycrystalline $x=0.4$ samples that $|\delta|$, "which was controlled by postannealing and quenching," was <0.005 using temperatures in the range of 600–1200 °C. For zone-growth boules, the thermal history of crystals depends on their position in the boule, i.e., the initial part cools continuously and slowly while the boule moves through the hot zone at ~6 mm/h, while the final part will experience a different history. This uncertainty can be mitigated by oxygen anneal-

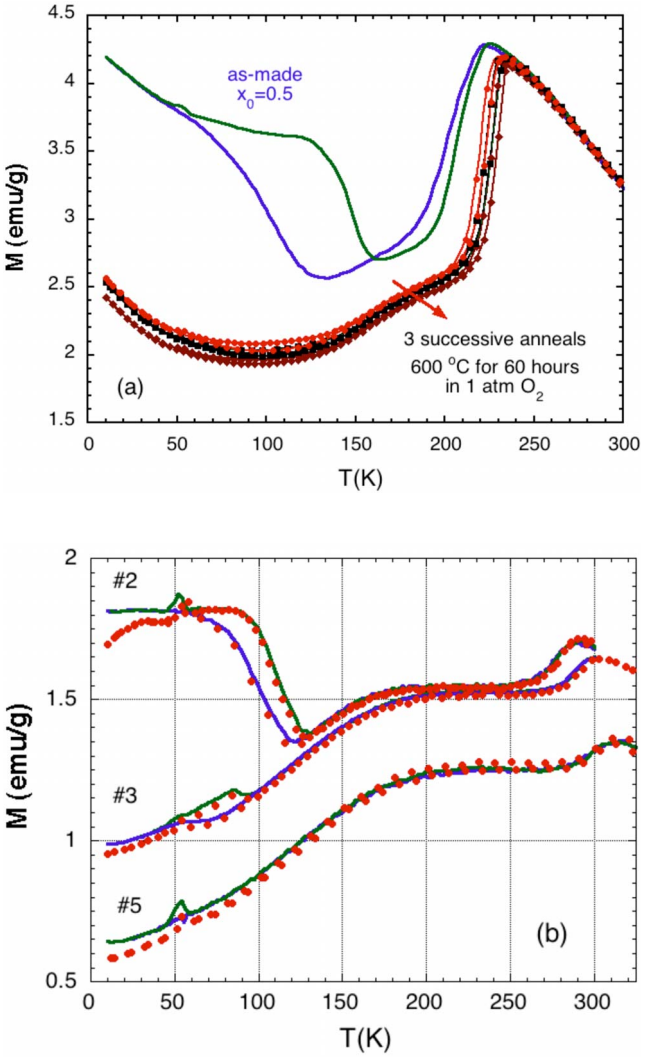

FIG. 3. (Color online) The effect of annealing in pure oxygen at 600 °C for 60 h followed by our slow-cooling protocol is shown on the magnetization (both heating and cooling) for (a) $x_0=0.5$ and (b) $x_0=0.61$. The magnetization in (a) for the as-made crystal (solid lines) is clearly re-entrant with hysteretic transitions from the PM to CO phases near 200 K and between the CO and AAFM phases centered at ~125 K. Upon annealing this crystal transformed into a non-re-entrant, predominantly CO phase down to the lowest temperatures (solid circles). Two further anneals (solid squares and diamonds) made much smaller changes, but in the same direction. From this data the oxygen deficiency of the as-made crystal, δ, can be estimated to be ~0.005. For samples 2, 3, and 5 from the nominal 0.61 boule of Fig. 2, the magnetic behavior (b) after annealing (solid circles) was barely distinguishable from the as-made crystals (solid lines) and δ is estimated (see text) to be an order of magnitude smaller at ~0.0003.

ing and we found dramatic differences in the conversion of a particular re-entrant crystal near $h_{CO}=0.5$ into a "pure" CO crystal. That conversion is shown in the magnetization data of Fig. 3(a), before annealing, and after each of three successive anneals. These postanneals are done in pure oxygen at 600 °C for 60 h followed by a slow-cooling protocol of 0.5 °C per minute that is expected to reduce δ and not change x (note that slow cooling at 0.1 °C per minute for the last of these anneals did not result in noticeably different effects). After the first anneal this crystal transforms into a non-re-entrant crystal, indicating h has become very close to 0.5, and that the as-made crystal had $h=x-\delta<0.5$. Subsequent anneals showed very small, additional changes implying that one such anneal *followed by our slow-cooling protocol* is sufficient to fill a large fraction of oxygen vacancies in as-grown crystals. From crystals made at neighboring compositions ($x_0=0.48$ and 0.52) and others made at $x_0=0.5$, we can estimate the width of the CO phase to be no larger than ± 0.01 and thus find δ to be $<\sim 0.005$ for the as-made crystal, and that is within the limits of quenched samples.[20]

Three crystals from the $x_0=0.61$ boule (2, 3, and 5) also underwent the same oxygen annealing and slow-cooling protocol. These data [Fig. 3(b)] indicate a barely discernable change, implying very few vacancies in the $x_0=0.61$ boule (unless vacancy filling for $x=0.61$ requires a radically different protocol). Using the very small temperature shifts in Fig. 3(b) and the transition temperature difference at the fixed points of $h=0.60$ and $x=0.61$, we estimate δ to be $<\sim 0.0003$. This small value of δ suggests that crystals 9–11 have hole doping, $h=0.61-\delta$, very close to 0.61. The reason for the much smaller effect in the as-made $x_0=0.61$ boule is not understood, but it could result from an x dependence of oxygen vacancy formation or on differences in the actual cool-down parameters *following zone growth* for the two boules.

The existence of crystals with re-entrant CO for h in the close vicinity of $h_{CO}=0.5$ or 0.6 certifies that the CO phase fields are broader in h at intermediate temperature than at low temperature. We present here a free-energy argument that qualitatively explains this experimental fact. Consider the free energy, $U-TS$, where U is the internal energy and S is the entropy, for four states: high-temperature paramagnet, competing low-temperature AAFM state, paramagnetic charge and orbital ordered state (CO PM), and finally the CO AFM state, e.g., with in-plane AF CE magnetic structure that is known[8,9] to exist for $h\sim 0.5$ below about 130 K. For simplicity of presentation, we neglect the temperature dependencies of U and S, and make the plausible assumption that only the U's of the CO states are strongly dependent on h with a symmetrical minimum at h_{CO}. The PM state has the least order and the highest entropy, so its $U-TS$ will exhibit the steepest negative slope versus temperature. The AAFM phase with FM monolayers may be expected to have the lowest entropy, and thus the flattest slope. Of the CO states the one with in-plane AF order has the lower entropy. The result of these considerations is shown in the bottom of Fig. 4, for a particular choice of U for each state, and is drawn assuming the CO states obey $U(h)-U(h_{CO})\propto|h-h_{CO}|$. Then the successive dashed (CO) curves from the bottom represent increasing $|h\text{-}h_{CO}|$. The solid squares (circles) indicate the lower (upper) limit of stability for the CO states, while the open circle indicates a direct transition from the AAFM to PM. The phase diagram at the top of Fig. 4 is the projection of these transition temperatures to their appropriate h values. Note however that these AAFM to CO transitions (squares) and CO to PM transitions (circles) are first order so significant hysteresis is expected and found[8,19] (see Figs. 3 and 8).

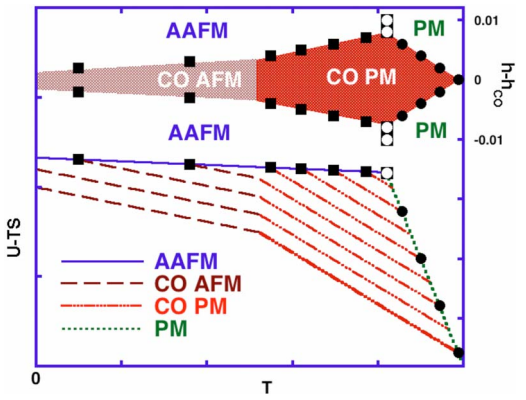

FIG. 4. (Color online) The proposed generic phase diagram for charge ordered phases in the bilayered manganites. The lower part represents the free energy by accounting for the differences in entropy, S, and internal energy, U, for the various phases, AAFM, CO AF, CO PM, and PM. Here U and S and assumed to be independent of T. The lowest dashed lines are for $h=h_{CO}$ (e.g., $h_{CO}=0.5$), while the next ones show sequentially increasing $|h-h_{CO}|$. The diagram specifically calls out the appearance of AF order in the CO phase (e.g., the known CE AF order at 0.5 doping). The upper diagram shows the transition points projected onto a phase diagram versus doping, h-h_{CO} (in arbitrary units).

Also, if AF order were frustrated in the CO state or occurred at the PM to CO transition, say for 0.6 doping, then the dashed lines in the lower part of Fig. 4 would be straight lines with no kinks, as would be the phase lines in the upper diagram from $T=0$ to the widest part of the CO phase.

As mentioned above, a high degree of crystal homogeneity is required to reveal the intrinsic behavior of bilayer manganites, and the path to homogeneity starts with crystal growth[21] in a floating-zone, optical image furnace. From the resulting boule, platelike crystals with the c axis normal are extracted and shaped ($\sim 2\times 0.5\times 0.1$ mm^3) so that four gold pads can be deposited along the top and bottom surfaces for six-terminal measurements[22] of the c axis, σ_c, and ab-plane, σ_{ab}, conductivity. To evaluate homogeneity, we determine and compare σ_{ab} and σ_c in four configurations (see methods A and B in the Appendix). For crystals very close to $h_{CO}=0.6$, the extraordinarily large anisotropy ($\sim 10^5$) at low temperatures renders the six-terminal data not useful. However, *for such high anisotropy*, combining two four-terminal measurements, the top voltage of method A and V_1 of method B, provides sufficiently accurate values of σ_{ab} and σ_c. For each four-terminal configuration, the results for currents applied to opposite sides of the crystal are compared to test homogeneity, and these data, presented in Fig. 5, are qualitatively identical and within a factor of 3, thus passing our criteria.[8]

It is of interest to compare the conductivity of pure CO crystals at $h_{CO}=0.60$ with re-entrant crystals with $h\sim 0.59$ and $h\sim 0.61$. Using the analysis described above,[22] extraordinarily low values of σ_{ab} and σ_c are reported here at low temperatures in the pure CO state, whereas the AAFM phases at $h\sim 0.61$ and[19] $h\sim 0.59$ show especially high metallic σ_{ab} at low temperatures. This contrast of greater than ten orders of magnitude is shown in Fig. 6. That it occurs for a 1% change in Sr content is remarkable and this contrast

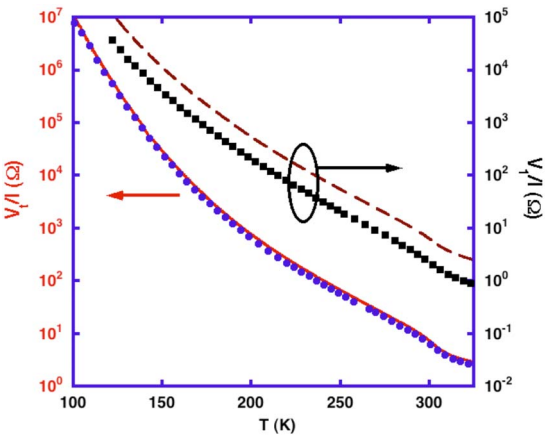

FIG. 5. (Color online) Homogeneity tests for a crystal with h very close to 0.60. In this case the qualitatively identical data from pairs of V_1 and of V_t represent the two configurations of each four-terminal measurement on opposite sides or ends of the crystal. In the worst case of V_1, the magnitudes are within a factor of 3.

also reaffirms the uniformity of doping in our crystals. Note however, we never found CO crystals for $h\sim 0.5$ without a small ($\sim 1-5\%$) contamination of the AAFM phase [Ref. 8 and Fig. 3(a)], but that is likely a result of the significantly narrower phase field for $h_{CO}=0.50$ and an inevitable small doping inhomogeneity.

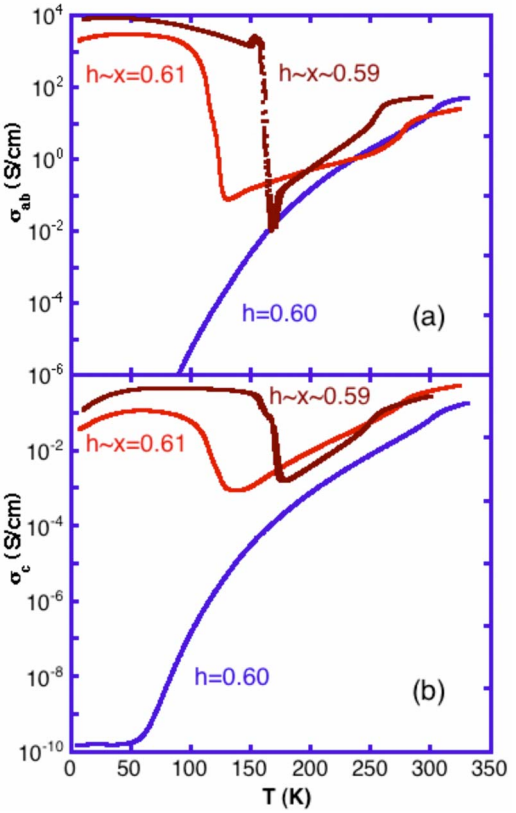

FIG. 6. (Color online) These data contrast the enormous conductivity ratio ($>10^{10}$) between a pure CO state at $h\sim 0.60$ and the low-temperature AAFM phase of re-entrant crystals for $h\sim 0.61$ and (Ref. 19) $h\sim 0.59$: (a) σ_{ab} and (b) σ_c. The flat behavior of σ_c below ~ 50 K is due to limitations of our measurement system.

The phase diagram in Fig. 1 begs some open questions. Can random doping yield such narrow needlelike phases? Random doping would require rather large volumes ($\sim$4000 unit cells $\sim 9^3$ nm^3) to achieve an *average* doping *within* the very narrow doping ranges ($\Delta h \sim \pm 0.005$) found at the lowest temperatures for $h \sim 0.5$. Thus obtaining phase purity with random doping addresses the Coulomb energy needed to homogenize the charge and that is conveniently discussed through a comparison of the electron screening length, r_s, with the needed 9-nm cell diameter from above. For manganites, r_s is not expected to be greater than values typical of semiconductors, i.e., 2–3 nm, so that locally inhomogeneous phases would be expected for random doping with $h \sim 0.5$. Given these estimates, it seems difficult to imagine that random doping could cause such an abrupt change in phase *uniformly* over the entire crystal for a 1% variation of *average h*, yet a high degree of uniformity has been verified with four independent bulk probes.[8] Cation ordering is one way to mitigate this issue. For $h=0.5$, on average, there is one La and two Sr per unit cell so there is a symmetrical occupancy with La only in the 12-coordinated site of the perovskite layer. The poor scattering contrast between La and Sr makes the determination of cation ordering particularly hard but it has been reported[23] for $x_0=0.4$ and 0.5 samples. In each case there is a higher-than-average La occupancy in the perovskite layer, but the 50% La enrichment found for 0.5 may be too small to completely mitigate the Coulomb energy.

The region of the phase diagram between these two needlelike phases is not fully resolved. One issue is the electronic nature of AAFM states. For nominal $x_0=0.58$ crystals[24] the extrapolated zero-temperature *ab*-plane conductivity is smaller than the data presented here for $h \sim 0.59$ and 0.61, but remains finite, i.e., metallic. For $h \sim 0.46$, much lower values of σ are seen[25] at intermediate temperatures with strongly insulating low-temperature behavior. For the AAFM states of crystals near nominal $h=0.5$, the intermediate-temperature conductivity values fall between these two extremes,[8] but insulating behavior is found at low temperatures. A possible scenario is a continuous *ab*-plane-metal-to-insulator transition as h decreases from $\sim$0.58 to $\sim$0.5. Note that the upper limit in h for the *ab*-plane metal is presently unknown. In the above picture CO *replaces* the AAFM over limited h ranges centered at 0.5 and 0.6 through first-order transitions, but the h dependence of the AAFM states may be otherwise unaffected.

A second issue is the continuous variation of the superlattice CO modulation over this doping range that was inferred[26] from the observed "incommensurate" superlattice in the bilayer manganite at $x_0=0.55$. A more complete set of "incommensurate" doping was reported for the *single-layer* manganites,[27] $La_{1-x}Sr_{1+x}MnO_4$, together with a strong argument supporting a charge-density wave (CDW) picture. Others[28] report a discontinuous jump in the superlattice peak for *bilayer manganites* between $h=0.5$ and 0.6. Our data strongly imply that CO in *bilayer manganites* at $h=0.5$ and 0.6 only exists over a finite doping range ($\Delta h \sim \pm 0.01-0.02$), as we find many crystals, at $x_0=0.52$, 0.54, 0.56, and[24] 0.58, that display a single transition in conductivity from a PM to an AAFM at low temperatures. Thus our data exclude the existence of continuous CO states from 0.5 to 0.6, although we have insufficient evidence to rule out, e.g., an additional CO phase at $h=0.55$ as reported in Ref. 26 (that would be necessarily needlelike). Each above issue needs a systematic doping study to establish the behavior of the $La_{2-2x}Sr_{1+2x}Mn_2O_{7-\delta}$ phase diagram between the needlelike CO phases at $h=0.5$ and 0.6.

Why is the CO at 0.6 more stable (higher T_{CO} and broader h range) than the highly symmetric checkerboard ordering[7] of Mn^{+3} and Mn^{+4} charges at 0.5 doping? A suggested picture of local charge (and orbital) ordering for $x=0.6$ adds an extra row of Mn^{+4} into the checkerboard pattern for every 5th row to achieve 0.6 doping in a so-called quasibistripe order.[28] This leads to a far less symmetrical pattern that one might expect to have a higher energy, and due to some frustrated AFM bonds, it also means that AFM will be less stable than the CE magnetic structure at $h=0.5$. In spite of the similar appearance of the needle-like phase fields, we now address the possibility that the CO state at $h \sim 0.6$ is not due to an arrangement of localized charges but more akin to a charge-density wave.

To start out, we find that the bilayer manganites behave differently to single-layer[27] and perovskite manganites in regard to CO states between $h=0.5$ and 0.6. The superlattice modulation wave vector, q, of the latter exhibit one of the following: (1) a broad continuous variation[29] of q starting above $\sim$100 K; (2) a narrow temperature dependence[30] of q near T_{CO} that could result from critical fluctuations; or (3) a broad transition starting at T_{AF} and extending[30] up to T_{CO}. All these have been discussed within a phenomenological CDW picture.[31] We find for the re-entrant *bilayer* with $h \sim 0.59$ that q is strictly temperature independent over its stability range (160–250 K), albeit its value of $\sim$0.21 is not commensurate.[19] The strong temperature dependencies of q in the perovskites are probably not consistent with a Fermi-surface nesting scenario for the CDW. However, at least some of these data might be understood as a commensurate-to-incommensurate transition[32] preceding the disappearance of CO at T_{CO}. In the bilayer, the very narrow range of stability ($h=0.6\pm0.02$) of the CO state would also seem to be at odds with any Fermi-surface nesting feature that might be expected to evolve more gradually with h. The question remains as to when and if the locked-in, low-temperature superlattice modulation is commensurate. In bilayer manganites, a broad temperature-dependent variation of q was also seen[28] for $x_0=0.575$ and 0.6 (but for $h=0.6$ the low-temperature $q \sim 0.2$ may be commensurate and is close to our value[19] of 0.21 for $h \sim 0.59$). That study[28] also found that $x_0=0.5$ and 0.55 exhibited temperature-independent $q \sim 0.25$, which is universally found and expected for checkerboard ordering at $h \sim 0.5$. This discussion reveals that there is much still to be learned about CO in the manganites.

In summary, our discovery of similar needlelike CO phases centered at $h=0.5$ and 0.6 drastically modifies the accepted picture of the bilayer manganite phase diagram. Compositional purity was crucial to our results and we ensured this by stringent testing of small ($\sim$1 mg) crystals. Phases were verified by observations with up to four bulk probes. The lack of sufficient purity could explain why others consistently report the lack of CO at low temperatures

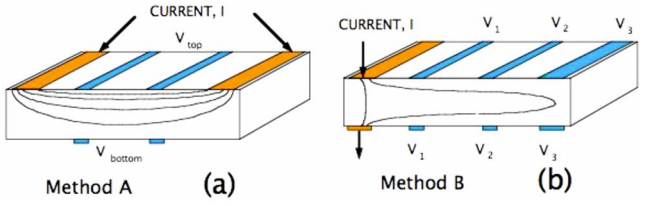

FIG. 7. (Color online) Schematic of six-terminal configurations for (a) method A and (b) method B.

and coexistence of CO and AAFM order in $LaSr_2Mn_2O_7$ (h=0.5). Open questions include: (1) whether the reported[23] cation order can overcome Coulomb energies and lead to such narrow phase fields; (2) why the CO state at h=0.6 is more stable than the checkerboard CO state at h=0.5; and (3) to what extent the CDW scenario may apply in the bilayer manganites.

ACKNOWLEDGMENTS

This research was supported by the U.S. Department of Energy, Basic Energy Sciences—Materials Sciences, under Contract No. DE-AC02-06CH11357. The authors wish to thank S. Rosenkranz and R. Osborn for ongoing, informative discussions and insights.

APPENDIX

In general, the principal components of conductivity, i.e., along the c axis, σ_c, and in the ab-plane, σ_{ab}, cannot be easily determined by four-terminal measurements so we commonly use six of the eight terminals to determine *each individually*. In transport method A, current is injected through the outermost contacts on one surface [Fig. 7(a)]. Laplace's equation is solved and inverted to get σ_{ab} and σ_c from voltages measured across the innermost contacts of each surface. In method B, Laplace's equation is solved for current injection through the top and bottom contacts at one end of the crystal, while voltages from the top to bottom of the crystal are measured between any two of the three pairs of remaining contacts [Fig. 7(b)].

To test for homogeneity, we evaluate σ_{ab} and σ_c in four configurations. Two use method A with current applied to the outer contacts of *either* the top or bottom surfaces and two use method B with current applied to the end contacts on either the right- or left-hand sides. We require both $\sigma_{ab}(T)$ and $\sigma_c(T)$ to be qualitatively the same for all four configurations and within a factor of 2–3 in magnitude. Crystal data reported in this paper all pass our criteria.[8,19] In Fig. 8 these homogeneity tests are shown for two re-entrant crystals near h_{CO}=0.5 used in Ref. 8 while similar data are shown in Fig. 2 of Ref. 19 for $h\sim0.59$.

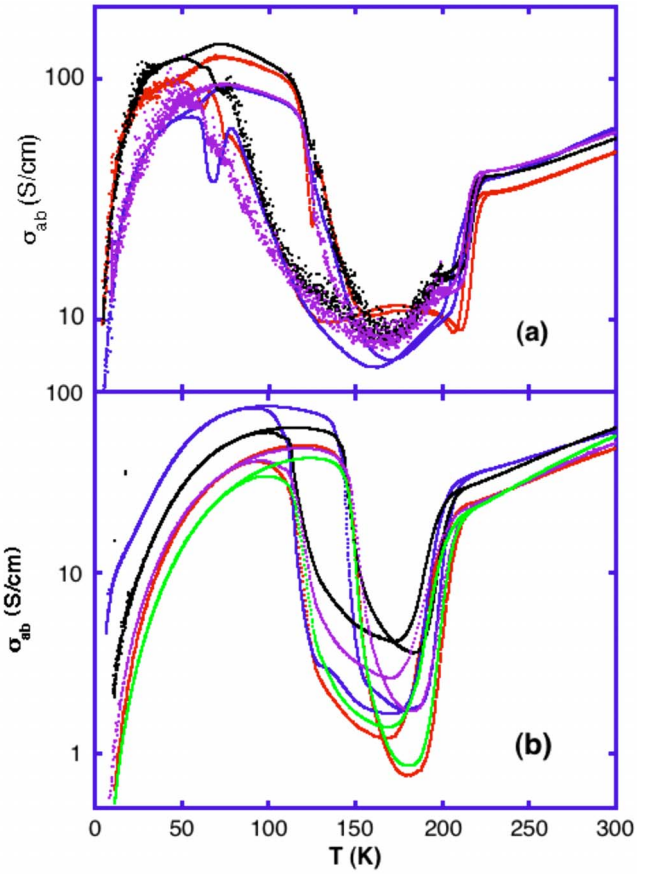

FIG. 8. (Color online) Homogeneity tests for σ_{ab} on two re-entrant crystals (Ref. 8) with x_0=0.5. The four sets of data for each crystal are comprised of two by method A (on both sides of crystal) and two by method B (at both ends of crystal). The hysteresis for each transition shows clearly they are of first order. The occasional sharp features are artifacts of slight inhomogeneity of the transition points along the length of the crystal and the abrupt change of σ_{ab} at the first-order transitions (note that the accompanying positive and negative peaks at around 70 K in the top curves dictate these features are not intrinsic). All data sets for each crystal are qualitatively very similar and within a factor of three in magnitude.

For crystals very close to h_{CO}=0.6, the extraordinarily large anisotropy ($\sim10^5$) at low temperatures render the six-terminal data not useful. In method A the bottom voltage is too small compared to noise and in method B the differences of voltages V_1 through V_3 are too small. However, combining two four-terminal measurements, the top voltage of method A and V_1 of method B, provides sufficiently accurate values of σ_{ab} and σ_c *when the anisotropy is so large*. In this case, our homogeneity test compares the results for each four-terminal configuration when currents are applied to opposite sides of the crystal. These data, presented above in Fig. 5, pass our criteria.

[1] S. Jin, T. H. Tiefel, M. McCormack, R. A. Fastnacht, R. Ramesh, and L. H. Chen, Science **264**, 413 (1994).
[2] Y. Moritomo, A. Asamitsu, H. Kuwahara, and Y. Tokura, Nature (London) **380**, 141 (1996).
[3] J. F. Mitchell, D. N. Argyriou, A. Berger, K. E. Gray, R. Osborn, and U. Welp, J. Phys. Chem. B **105**, 10731 (2001).
[4] B. J. Campbell, R. Osborn, D. N. Argyriou, L. Vasiliu-Doloc, J. F. Mitchell, S. K. Sinha, U. Ruett, C. D. Ling, Z. Islam, and J. W. Lynn, Phys. Rev. B **65**, 014427 (2001).
[5] L. Vasiliu-Doloc, S. Rosenkranz, R. Osborn, S. K. Sinha, J. W. Lynn, J. Mesot, O. H. Seeck, G. Preosti, A. J. Fedro, and J. F. Mitchell, Phys. Rev. Lett. **83**, 4393 (1999).
[6] R. Osborn, S. Rosenkranz, D. N. Argyriou, L. Vasiliu-Doloc, J. W. Lynn, S. K. Sinha, J. F. Mitchell, K. E. Gray, and S. D. Bader, Phys. Rev. Lett. **81**, 3964 (1998).
[7] J. B. Goodenough, Phys. Rev. **100**, 564 (1955).
[8] Q. A. Li, KE. Gray, H. Zheng, H. Claus, S. Rosenkranz, S. N. Ancona, R. Osborn, JF. Mitchell, Y. Chen, and J. W. Lynn, Phys. Rev. Lett. **98**, 167201 (2007).
[9] M. Kubota, H. Yoshizawa, Y. Moritomo, H. Fujioka, K. Hirota, and Y. Endoh, J. Phys. Soc. Jpn. **68**, 2202 (1999).
[10] C. D. Ling, J. E. Millburn, J. F. Mitchell, D. N. Argyriou, J. Linton, and H. N. Bordallo, Phys. Rev. B **62**, 15096 (2000).
[11] D. N. Argyriou, H. N. Bordallo, B. J. Campbell, A. K. Cheetham, D. E. Cox, J. S. Gardner, K. Hanif, A. dos Santos, and G. F. Strouse, Phys. Rev. B **61**, 15269 (2000).
[12] T. Chatterji, G. J. McIntyre, W. Caliebe, R. Suryanarayanan, G. Dhalenne, and A. Revcolevschi, Phys. Rev. B **61**, 570 (2000).
[13] T. Kimura, R. Kumai, Y. Tokura, J. Q. Li, and Y. Matsui, Phys. Rev. B **58**, 11081 (1998).
[14] Y. Wakabayashi, Y. Murakami, I. Koyama, T. Kimura, Y. Tokura, Y. Moritomo, Y. Endoh, and K. Hirota, J. Phys. Soc. Jpn. **72**, 618 (2003).
[15] S. B. Wilkins, P. D. Spencer, T. A. W. Beale, P. D. Hatton, M. v. Zimmermann, S. D. Brown, D. Prabhakaran and A. T. Boothroyd, Phys. Rev. B **67**, 205110 (2003).
[16] Y. Tomioka and Y. Tokura, in *Colossal Magneto-Resistive Oxides*, edited by Y. Tokura (Gordon and Breach, Amsterdam, 2000), Chap. 8.
[17] That the melt is Sr rich compared to the growing crystal is known empirically. See also W. G. Pfann, *Zone Melting*, 2nd ed. (Wiley, New York, 1966), pp. 27–31.
[18] X. J. Chen, C. L. Zhang, J. S. Gardner, J. L. Sarrao, and C. C. Almasan, Phys. Rev. B **68**, 064405 (2003).
[19] Q. A. Li, K. E. Gray, S. N. Ancona, H. Zheng, S. Rosenkranz, R. Osborn, and J. F. Mitchell, Phys. Rev. Lett. **96**, 087201 (2006).
[20] J. Shimoyama, Y. Yokota, M. Shiraki, Y. Sugiura, S. Horii, and K. Kishio, in *Solid-State Chemistry of Inorganic Materials V*, edited by Jing Li, Nathaniel E. Brese, Mercouri G. Kanatzidis, and Martin Jansen, MRS Symposia Proceedings No. 848 (Materials Research Society, Warrendale, PA, 2005), p. 523.
[21] J. F. Mitchell, D. N. Argyriou, J. D. Jorgensen, D. G. Hinks, C. D. Potter, and S. D. Bader, Phys. Rev. B **55**, 63 (1997).
[22] Q. A. Li, K. E. Gray, and J. F. Mitchell, Phys. Rev. B **59**, 9357 (1999).
[23] R. Seshadri, M. Hervieu, C. Martin, A. Maignan, B. Domenges, B. Raveau, and A. N. Fitch, Chem. Mater. **9**, 1778 (1997); P. D. Battle, M. A. Green, N. S. Laskey, J. E. Milburn, L. Murphy, M. J. Rosseinsky, S. P. Sullivan and J. F. Vente, *ibid.* **9**, 552 (1997).
[24] E. Badica, K. E. Gray, J. F. Mitchell, and H. Zheng, Phys. Rev. B **70**, 174435 (2004).
[25] Q. A. Li, K. E. Gray, A. Berger, and J. F. Mitchell, Phys. Rev. B **67**, 184426 (2003); N.B. The crystal used in this study was originally designated by x_0=0.48, but extensive recent studies using boules made nominally at x_0=0.48 and 0.46 lead us to believe it was actually closer to 0.46.
[26] J. Q. Li, C. Dong, L. H. Liu, and Y. M. Ni, Phys. Rev. B **64**, 174413 (2001).
[27] S. Larochelle, A. Mehta, N. Kaneko, P. K. Mang, A. F. Panchula, L. Zhou, J. Arthur, and M. Greven, Phys. Rev. Lett. **87**, 095502 (2001).
[28] T. A. W. Beale, P. D. Spencer, P. D. Hatton, S. B. Wilkins, M. v. Zimmerman, S. D. Brown, D. Prabhakaran, and A. T. Boothroyd, Phys. Rev. B **72**, 064432 (2005).
[29] J. C. Loudon, S. Cox, A. J. Williams, J. P. Attfield, P. B. Littlewood, P. A. Midgley, and N. D. Mathur, Phys. Rev. Lett. **94**, 097202 (2005).
[30] C. H. Chen, S. Mori, and S. W. Cheong, Phys. Rev. Lett. **83**, 4792 (1999).
[31] G. C. Milward, M. J. Calderon, and P. B. Littlewood, Nature (London) **433**, 607 (2005).
[32] J. C. Toledano and P. Toledano, *The Landau Theory of Phase Transitions* (World Scientific, Singapore, 1987), Chap. V.